

DESY SR 84-18
May 1984

INTRAMOLECULAR BAND MAPPING OF POLY(p-phenylene) BY
UV PHOTOELECTRON SPECTROSCOPY OF SEXIPHENYL

Eigenname	_____	_____
Property	_____	_____
Zurück	- 4. JUL 1984	_____
Accession	_____	_____
Leihfrist:	7	days
Loan period:	7	days

by

K. Seki

Hamburger Synchrotronstrahlungslabor HASYLAB at DESY
and
Institute f. Molecular Science, Myodaiji, Okazaki

U.O. Karlsson

Hamburger Synchrotronstrahlungslabor HASYLAB at DESY
and
Dept. of Physics & Measurement Technology, Linköping University

R. Engelhardt

II. Institut f. Experimentalphysik, Universität Hamburg

E.-E. Koch

Hamburger Synchrotronstrahlungslabor HASYLAB at DESY

W. Schmidt

Biochemisches Institut f. Umweltcarcinogene, Ahrensburg

ISSN 0723-7979

NOTKESTRASSE 85 · 2 HAMBURG 52

DESY behält sich alle Rechte für den Fall der Schutzrechtserteilung und für die wirtschaftliche Verwertung der in diesem Bericht enthaltenen Informationen vor.

DESY reserves all rights for commercial use of information included in this report, especially in case of filing application for or grant of patents.

To be sure that your preprints are promptly included in the
HIGH ENERGY PHYSICS INDEX ,
send them to the following address (if possible by air mail) :

DESY
Bibliothek
Notkestrasse 85
2 Hamburg 52
Germany

Intramolecular Band Mapping of Poly(p-phenylene) by

UV Photoelectron Spectroscopy of Sexiphenyl*

Kazuhiko SEKI

Hamburger Synchrotronstrahlungslabor HASYLAB at DESY and
Institute for Molecular Science, Myodaiji, Okazaki 444, Japan

Ulf O. KARLSSON

Hamburger Synchrotronstrahlungslabor HASYLAB at DESY and
Department of Physics and Measurement Technology, Linköping University,
S-58183 Linköping, Sweden

Rainer ENGELHARDT

II. Institut für Experimentalphysik, Universität Hamburg,
D-2000 Hamburg 50, Federal Republic of Germany

Ernst-Eckhard KOCH

Hamburger Synchrotronstrahlungslabor HASYLAB at DESY,
D-2000 Hamburg 52, Federal Republic of Germany

and

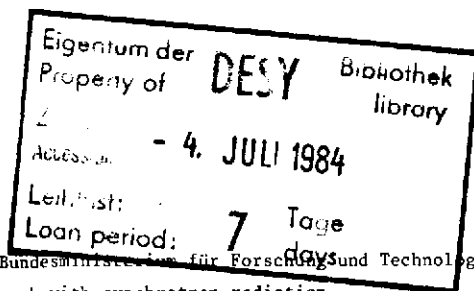
Werner SCHMIDT

Biochemisches Institut für Umweltcarcinogene,
D-2070 Ahrensburg, Federal Republic of Germany

Abstract

Ultraviolet photoelectron spectra were measured of solid sexiphenyl with synchrotron radiation and of gaseous polyphenyls from biphenyl to sexiphenyl with a HeI light source. The similarity of the spectrum from the solid with the XPS spectrum of poly(p-phenylene) (PPP) shows the usefulness of sexiphenyl as a model compound of PPP. Examination of the fine structure observed in the low binding energy region clearly shows how the electronic structure of the p-phenylenes evolves from that of benzene, including the effects of deeper levels and of the non planarity of the molecular geometry. The experimental $E = E(k)$ energy band dispersion relation of a PPP chain can be deduced by giving each energy level of the oligomers an appropriate k value. An extrapolation for the total band width and the threshold photoemission energy of solid PPP yields $3.9_{\pm 0.1}$ eV and $6.6_{\pm 0.1}$ eV, respectively.

submitted to Chem. Phys.



* Work supported in part by Bundesministerium für Forschung und Technologie (BMFT) from funds for research with synchrotron radiation.

1. Introduction

Recently the electronic structure of poly-p-phenylene (PPP) has attracted considerable interest owing to its high conductivity in the presence of dopants [1]. Several theoretical papers have been published on the band structure of a PPP chain [2-6]. Also several workers [6-9] reported calculations on oligomers such as biphenyl, p-terphenyl, and p-quarterphenyl, and discussed the change in the transition from benzene to the infinite PPP chain. Riga et al. [9] used X-ray photoelectron spectroscopy (XPS) to study the valence band structure and the shake-up features of the core levels for PPP and oligomers up to p-quarterphenyl. The XPS data for the valence band were explained fairly well by the calculations of Brédas et al. [5] and Boutique et al. [7].

However, several problems still remain. The photoemission cross sections of C 2p derived orbitals at XPS energies are small, and the decreased sensitivity has hampered a detailed study of the uppermost π -levels of the valence bands, which are most important in discussing the electronic conduction. This raises questions such as (1) what is the degree of delocalization of π -electrons [9,10], (2) how does the energy structure depend on the number of the rings n [6,9], (3) how does the suggested deviation from a coplanar molecular geometry affect the electronic structure [6], and even (4) can the uppermost π levels be resolved at all in photoelectron spectra from solid samples [6]? As for (1), Creelius et al. [10] reported angle-resolved electron energy-loss spectra, but this technique provides information concerning excitons (bound electron-hole pairs) and not on the delocalizability of valence electrons in the ground state. Since ultraviolet photoelectron spectroscopy (UPS) is more sensitive for C 2p derived orbitals and generally yields higher resolution than XPS, an UPS examination of the valence bands is highly desirable [6].

Further, the physical characterization of PPP is difficult owing to problems characteristic for polymers, e.g. cross-linking, chain branching [11], and incomplete knowledge of chain length or molecular geometry. Fortunately, Ford et al. [6] reported that there is no substantial change in electronic structure as the chain is extended beyond p-quarterphenyl ($n=4$) to an infinite chain. This suggests that we can use an oligomer of reasonable length as a well-defined model compound of PPP. Another advantage of oligomers compared to a polymer in UPS experiments is that often thin and uniform films can be

prepared as samples by vacuum evaporation or casting from solution, neither of which is applicable to PPP. With such good samples, the absolute energy of levels can be determined without problems of sample charging.

However, the UPS studies have so far been limited to short molecules such as biphenyl ($n=2$) [12] and p-terphenyl ($n=3$) [13]. These molecules are not long enough to simulate PPP, although the analysis of their electronic structures showed how the π -levels of the benzene rings interact to form the orbitals of these molecules.

In this paper, we report results from an UPS study of a long model compound, sexiphenyl ($n=6$), in the solid and gaseous state, as well as gas phase spectra of shorter oligomers. We analyze our results with the aid of theoretical band structure calculations [5,6] and in comparison to XPS results [9]. We were able to resolve the uppermost π -bands clearly, even in the spectra from the solid films. Their fine structure vividly shows, how π -bands are formed from the π -orbitals of benzene. Thus we are able to deduce an experimental energy band dispersion relation $E = E(k)$. Furthermore, by comparing the gas phase and solid state results, we assess (1) the effects of nonplanarity of the molecular geometry, and (2) the lowering of the ionization energy by molecular aggregation (polarization energy) [14].

2. Experimental details

2.1 UPS from solid films of sexiphenyl

Sexiphenyl was purchased from K&K Co. Inc.. The material was purified by vacuum sublimation. The sample was prepared as a thin film of ~ 7 nm thickness by in situ evaporation on a Cu substrate in an ultra-high-vacuum (UHV) preparation chamber with a base pressure of 5×10^{-10} Torr. It was subsequently transferred to the photoelectron spectrometer under UHV. Before evaporation the sexiphenyl was outgassed at elevated temperatures. The photoelectron spectra were measured with a set-up described previously [15], consisting of a 1 m Seya-Namioka monochromator and a modified VG ADES 400 angle-resolving photoelectron spectrometer. Synchrotron radiation from the storage ring DORIS II at DESY was used as the light source. The absolute binding energy relative to the vacuum level was calibrated by independent measurements with $h\nu \sim 8$ eV, using a retarding-potential-type photoelectron spectrometer described previously [16].

2.2 UPS from gaseous polphenyls

The HeI spectra were measured with a model "0078" Photoelectron Spectrometer of PES Ltd., High Wycombe, England, using a light source provided by Helectros Developments, Beaconsfield, England. Calibration of the spectra was performed in situ as described in ref. [40]. The spectral resolution was set at 18 meV for the Ar $2P_{3/2}$ peak.

To monitor the possible occurrence of impurities, the spectra were recorded at slowly increasing temperatures until no further change was observed. Biphenyl was sufficiently volatile at room temperature, so that no heating of the ionization chamber was required. Optimum temperatures for the higher homologs were as follows: p-terphenyl 120°C, p-quarterphenyl 195°C, p-quinquephenyl 250°C, p-sexiphenyl 294°C.

3. Results and Discussion

In Figure 1(a) a wide scan UPS spectrum of solid sexiphenyl for a photon energy $h\nu = 33$ eV is shown. The corresponding gas phase HeI spectrum of sexiphenyl is shown in Fig. 2(a), together with spectra of shorter molecules (b)-(f). The two spectra are quite similar, although there are some differences which will be discussed later. We will first discuss the overall structure of the valence band in the spectrum from the solid film which covers the whole valence band.

The spectrum in Fig. 1(a) was measured with a setting of $\alpha = 70^\circ$ and $\theta = 0^\circ$, where α is the angle of incidence of the photons and θ is the emission angle of electrons, both measured from the normal to the surface. The electric vector of the polarized synchrotron radiation was in the plane of incidence.

Previous spectra of oriented crystalline samples of another long-chain molecule compound, $n\text{-CH}_3(\text{CH}_2)_{34}\text{CH}_3$, showed a drastic dependence on $h\nu$, α , and θ , both in peak positions and peak intensities [17,18], from which we have determined the intramolecular energy band dispersion [18]. In the present case, however, the spectra did not show any significant dependence on these parameters except that the bands A-F became weaker for large values of α . This insensitivity may be due to the random orientation of molecules or microcrystallites in the specimen. As a result, we can regard the spectrum as reflecting the density of the valence states (DOVS).

For comparison, Fig. 1 also depicts (b) the previously reported XPS spectrum of PPP by Riga et al. [9], (c) the DOVS for planar PPP and p-quarterphenyl calculated with the CNDO/S3 method and broadened with a half width $\delta = 0.7$ eV to simulate the solid UPS spectrum [6], (d) the DOVS for a slightly twisted PPP calculated with the valence-effective-Hamiltonian (VEH) method, also broadened with $\delta = 0.7$ eV [5], and (e) the DOVS for planar p-quarterphenyl calculated with an ab-initio calculation, broadened with $\delta = 1.5$ eV [7]. Since the original binding energy scale of the XPS spectrum is relative to the Fermi level, the spectrum is shifted to align peaks D and F'. This corresponds to a work function of 4.5 eV. The DOVS in (d) corresponds to the choice of two phenyl groups per unit cell where adjacent phenyl rings are rotated by a twist angle of $\phi = 22.7^\circ$. This is the molecular conformation suggested by the crystal structure of p-quarterphenyl in the low-temperature phase [19]. It is further 1.3 times contracted in energy scale and corrected for the photoionization cross section at the Al-K $_{23}$ XPS energy [5]. The DOVS in (d) is also 1.34 times contracted and corrected for the photoionization cross section [6]. For all calculations (c) - (e), the energy scale is shifted to align the peak D in (a) with the corresponding peak in the DOVS.

Two comments are useful in discussing Fig. 1. First, there is a difference due to the state of aggregation, between the observed solid state photoelectron spectra (a and b) and theoretical calculations on an isolated chain (c to e). However, it is known that the photoelectron spectrum of a molecular solid agrees with that of a molecule when allowance is made for a shift in the energy scale [14,20,21]. Hence we can directly compare the observed spectra with calculated DOVS by adjusting the energy scales. Second, both CNDO/S3 [6] and VEH [5] methods indicate that the DOVS does not change drastically in the possible range of twist angles $0^\circ \leq \phi \leq 23^\circ$ in the solid polyphenylenes. Thus we can neglect the effect of molecular geometry in the discussion of the gross features of the valence bands (for details of the ϕ -dependence see below).

The overall agreement of the peak energies in the UPS and XPS spectra Figs. 1(a) and 1(b) is fairly good. This agreement verifies the theoretical prediction that sexiphenyl is a good model compound for PPP, which is illustrated by the small change in the DOVS between $n = 4$ and ∞ in Fig. 1(c) [16]. The binding energies of the peaks in both spectra are listed in Table 1, together with the assignment of the XPS peaks by Brédas et al. [5]. For the symmetry assignment the long axis and short axis have been chosen to be z and y respectively. The corresponding values for the gas phase spectrum (Fig. 2(a)) are also listed.

We also note differences between Figs. 1(a) and 1(b): (i) the relative peak intensities are very much different, and (ii) more fine structure is observed in the low binding energy region of the UV-spectrum compared to the X-ray spectrum. The variation in the relative intensities is due to the larger photoionization cross section for the C 2p derived orbitals compared to that of C 2s derived orbitals at low excitation energies (UPS) [5,9]. The states at low binding energies derived from C 2p orbitals are drastically enhanced in intensity in UPS as compared to XPS, while the highest binding energy peak A' in XPS, which corresponds to the bonding C 2s levels [5,7], could not be observed in UPS even at photon energies higher than 33 eV. A similar disappearance of the C 2s bonding peak in UPS was also observed in polyethylene and its model compounds [17]. The examination of the intensity variation suggests that maxima N, K, and J have more C 2p character than the maxima O, L, and I, respectively. Riga et al. [9] also noted the increasing 2p character of peak K with increasing chain length of oligomers. The present results are consistent with the assignment by Breddas et al. [5], except that the assignment of M is not clear.

Having discussed the gross features of the valence band, we will now examine the lower binding energy region in more detail. Theoretical calculations [5-7,9] assign this region to two pairs of π -bands. In Figure 3 solid and gas phase spectra of sexiphenyl are shown in this region. The gas phase spectrum is shifted by 1.0 eV towards lower binding energies in order to achieve alignment of peak D. This shift corresponds to the polarization energy [15], which will be discussed later.

We can assign the features in the spectra displayed in Fig. 2 by using the "composite molecule" model, which has already been applied successfully to biphenyl [12] and p-terphenyl [13]. In this simple model, we treat a polyphenyl molecule as consisting of n interacting benzene subunits with the uppermost levels derived from the degenerate e_{1g} π -orbitals of benzene. That is, we neglect the effect of other (lower) orbitals for the moment, because the e_{1g} orbitals are fairly well separated from the others in energy. Assuming the carbon atoms of the polyphenyls to lie in the y,z plane, with z being the long axis of the molecules, then one of the e_{1g} orbitals ($1a_2$ in the reduced point group C_{2v}) has a node and thus zero electron density at the point of substitution. Consequently it remains unaffected in polyphenylenes, forming non-bonding states. The other π -orbital of benzene ($2b_1$ in C_{2v} symmetry) brings about large inter-phenyl-moiety overlap leading

to a large splitting [6,12,13,22]. When we take account of the nearest-neighbour interaction only, the resultant energies of n interacting orbitals are given, in analogy to the well known [23] closed formula for linear polyenes, as

$$E_m = \alpha + 2\beta \cos\left(\frac{m\pi}{n+1}\right), \quad m = 1, 2, \dots, n \quad (1)$$

where α is the energy of an unperturbed e_{1g} state, and β is the interaction between neighbouring orbitals. When the linear chain is extended to infinite chain length, we get a pair of non-bonding bands with energy α and a pair of bands with an energy dispersion [24]

$$E(k) = \alpha + 2\beta \cos(ak/2), \quad (0 \leq k \leq \pi/a), \quad (2)$$

where a is the distance between the centers of the neighbouring rings and k is the wave vector. The resultant π -energy level scheme is shown in Fig. 4. For later discussion, we note that the orbital energies of a pair of symmetrically split levels of an oligomer are obtained from Eq. (2) by putting

$$k = \frac{2m\pi}{a(n+1)}, \quad (3)$$

where m runs from 1 to the maximum integer not exceeding $n/2$. Using this relation, we can locate the energy levels of an oligomer in the $E = E(k)$ dispersion of the polymer.

Comparison of Fig. 3 with Fig. 4 yields a straightforward assignment of the gas phase UPS spectrum of sexiphenyl. Inspection of figure 4 shows that the non-bonding orbitals form a large central peak in the DOVS. Peak D corresponds to these orbitals. Peaks A, B, C, E, F, and G correspond to the split orbitals. Similar assignments on biphenyl and p-terphenyl have already been reported [12,13]. Further, the complete set of peak energies in the spectra of the free (gas phase) molecules from benzene to sexiphenyl (in Fig. 2) is summarized in Fig. 5. There is an excellent agreement with the data shown in Fig. 3, which clearly demonstrates the essential correctness of this model. The shift of the deeper-lying σ levels with n can also be seen. We mention in passing that a similar pair of experimental and theoretical diagrams, showing the evolution of energy bands, has also been reported for the C 2s orbitals of normal alkanes [25].

In figure 6(a) we show a comparison of the simple model with the observed energy levels of oligomers in the gas and solid phases. k -values for the experimental results are given by Eq. (3). The theoretical curves were drawn using Eq. (2) with parameters $\alpha = 9.1$ eV and $\beta = 1.0$ eV (solid) or 0.8 eV (gas). The smooth curves given by the observed energy levels verify the basic idea of the simple model. However, the quantitative agreement is not so good. In particular, only one level can be seen in the high-binding-energy branch of the solid spectrum, and the splitting is larger in the solid state than in the gas phase.

For discussing these points, we must take into account (1) the possible nonplanarity in the molecular geometry, and (2) the effects of deeper-lying orbitals. The phenyl groups of *p*-phenylene oligomers in the gas phase are considerably twisted ($\phi = 42^\circ$ or 45° for biphenyl [27]) around the molecular axis, owing to the repulsion between the ortho hydrogen atoms. In the crystalline state at room temperature, the molecule becomes approximately planar as a result of an averaging effect of large-amplitude twisting thermal oscillations in a double-minima potential [26-29]. At low temperature (~ 110 K), this oscillation is frozen through a phase transition within one of these minima, and adjacent phenyl rings are twisted by $\phi = 16 - 25^\circ$ for *p*-terphenyl [30,31] and $17.1 - 22.7^\circ$ for *p*-quarterphenyl [19]. Hence we can expect that a sexiphenyl molecule is also nearly planar in the crystalline state at room temperature, while it is substantially twisted in the gas phase. This kind of twisting decreases the conjugation and splitting among π -orbitals of phenyl moieties.

The effects of nonpolarity and of deeper-lying orbitals on the uppermost valence levels can be examined by MO calculations including all valence electrons for various geometries. Unfortunately, such calculations are not available for long oligomers.

Nevertheless, we can discuss these effects by using the band calculations of an infinite polymer chain for various values of ϕ . Such an analysis also sheds light on the correlation of the electronic structure of the polymer with that of oligomers. In figures 6(b) and 6(c) the $E = E(k)$ dispersion relations of PPP are shown as calculated by CNDO/S3 ($\phi = 0^\circ$ and 23°) [6] and VEH ($\phi = 0^\circ$, 22.7° , and 42°) [5], respectively. The unit cell contains two phenyl groups. Different from Fig. 1(d), the energy scale of the VEH calculation is not contracted. The numbering of the bands is the same as in ref. [5]. The bands 13 - 13' and 14 - 14' correspond to the n -states discussed in the simple model.

For locating the observed energy levels of oligomers in these $E = E(k)$ diagrams, we assume that we can still use Eq. (3). This method was also used for deducing the $E = E(k)$ relation of the π -band of polyacetylene from the calculated orbital energies of polyene oligomers [32]. The validity of this method is illustrated by plotting the calculated CNDO/S3 energy levels of biphenyl ($\phi = 0^\circ$ and 23°) [6] in Fig. 6(b). The agreement including the ϕ dependence is excellent.

In Fig. 6(c), the experimentally observed energy levels including the c -levels are plotted with appropriate energy shifts for the best fit for the gas phase and solid state, respectively. We can regard this plot as the experimentally observed $E = E(k)$ dispersion relation. One can see from Fig. 6(c) that the trend of this relation is well reproduced even with the data of sexiphenyl only. Since the qualitative trend of both the CNDO/S3 and the VEH band calculation is similar, we will first analyze the experimental results using the VEH calculation, which gives a slightly better quantitative agreement. We will compare other calculations later.

The data of solid sexiphenyl are well described by the $E = E(k)$ curve for $\phi = 0^\circ$ in Fig. 6(b). This is consistent with the nearly planar molecular geometry as discussed above, although it is difficult to evaluate the precise value of ϕ from the present data. The observed spectral features A, B, C, and F fit fairly well with the curve. The absence of E can be ascribed to the overlap with the intense peak D (of the band 14 - 14' with the band 13 + 13' at $k = \pi/a$). Note that the FWHM of the solid spectrum is ~ 0.5 eV and that C is barely resolved from D. Similarly, G is obscured by the overlap with H, which also overlaps with deeper levels in band 10' and 12' to form the tail at the low binding energy side of peak I in Fig. 1(a).

The good agreement with theory and experiment allows us to extrapolate the experimental data of band 13' to $k = 0$, which corresponds to the highest occupied state of PPP. This gives a value of 6.10 eV on the solid state binding energy scale. The widths of the delocalized π -bands 13 and 13' can be estimated to be 1.9 ± 0.1 and 2.0 ± 0.3 eV, respectively. The large estimated error in the latter value is due to the difficulty in extrapolating band 13.

The width of band 13 corresponds to the lowering of the ionization energy from benzene due to the interaction of phenyl rings. For hexacene [33] and diphenylethane [34], the corresponding values derived from UPS are 2.81 eV

and 0.1 eV, respectively. Comparison of these values with the present value of 1.9 eV offers quantitative confirmation for the conclusion of Riga et al. [9] based on XPS results that the degree of delocalization in polyphenylenes is intermediate between the polyacenes and polystyrene. A more detailed discussion of polystyrene will be reported elsewhere [35].

The agreement of the gas phase data with the curves in Fig. 6(c) is not as good as that for solid sexiphenyl. This may be due to the different molecular geometry assumed in the calculation versus the prevailing situation in a gas phase experiment. Random twisting will occur at each single bond connecting the phenyl groups in the gas phase, while a regular repeat of a unit cell, containing two phenyl groups, was assumed in the calculation.

Nevertheless, important trends of the gas phase spectra can be explained by the curves for $\phi \neq 0^\circ$ in Fig. 6(c). As ϕ increases, the width of both bands 13 and 13' decreases. This explains the observed smaller splitting for sexiphenyl in the gas phase compared to the solid state. The larger decrease in 13 than in 13' and the shift of the band 14 - 14' from the location of 13 + 13' at $k = \pi/a$ result in an asymmetry relative to band 14 - 14' (peak D). Further, the decrease of the bandwidth of band 13 removes the overlap with band 10' and leads to a gap between these bands. It is clearly seen in the gas phase spectrum in Fig. 2(a). As a result, peaks G and H can be observed distinctly.

The extrapolation of the observed values of band 13' to $k = 0$ indicates that the deviation from planarity increases the binding energy of the highest occupied level of PPP by about 0.2 eV.

After the discussion of the intramolecular delocalization using adjusted energy scales, we will now consider the absolute binding energies and their dependence on the ring number n . The peak energies of gas phase spectra are compiled in Fig. 5. It is interesting to note that the energy of the central peak due to bands 14 + 14' is constant from benzene to sexiphenyl within 0.2 eV, as predicted by the simple theory, the extended Hückel- [9], CNDO/S3- [6], and VEH- [5] calculations. Since the energy of this peak is insensitive to twisting (see Figs 6(b) and 6(c)), we can safely say that the binding energy of this peak does not depend on the ring number or on the molecular geometry.

In Table 2 the binding energies of thresholds and peaks of solid benzene [36], p-terphenyl [13], and p-sexiphenyl are compared with the corresponding data for the gas phase. The gas to solid shifts of the adiabatic ionization energies P_+ and those of the peak energies R_+ are also listed. We note that the energy of the main peak for the solid phase is again fairly constant.

As mentioned above, the lowering of the ionization energy in going from the gaseous to the solid state is mainly caused by the electronic polarization of surrounding molecules to screen the photoionized molecule in the solid. We discussed previously that P_+ rather than R_+ should be used as the experimental value for the polarization energy of a molecule in the solid [14]. In going from benzene to p-sexiphenyl the value of P_+ in Table 2 changes from 2.1 to 1.3 eV, while the change of R_+ is much smaller. The observed values of P_+ for benzene and sexiphenyl deviate from the common value of ~ 1.7 eV [14] found for a wide range of aromatic hydrocarbons, but the value of R_+ is comparable with the value of ~ 1.1 eV for other compounds [14]. For sexiphenyl, the long molecular shape may be the reason for the small P_+ value.

In Table 2 are also listed estimated values for the highest occupied state of PPP. The peak energies of the coplanar solid and the twisted free molecule were estimated by the extrapolation shown in Fig. 6(c) as outlined above, and those of the coplanar free molecule and the twisted solid were deduced by assuming a contribution of 0.2 eV due to nonplanarity. The threshold values were calculated using the peak-threshold differences of sexiphenyl.

The estimated solid threshold agrees fairly well with the estimate of Shaklett et al. for PPP (5.5 eV) cited in ref. [5]. This value is larger than the threshold of trans-polyacetylene (5.28 eV) [37]. This difference is consistent with the observation that trans-polyacetylene becomes conducting on doping with a weak acceptor such as iodine [38], while PPP needs stronger acceptors [1].

Finally we will examine the agreement of various theoretical methods with the experimental results. In Table 3 are listed the uppermost π -bandwidth (13 + 13') and the energy of the highest occupied state of PPP obtained by various methods of calculation, which give reasonable results for the π -bands. The values of the ab-initio calculation were estimated from the results for p-quarterphenyl by multiplying with a factor according to the

simple model illustrated in Fig. 4. In Table 3 are also listed the experimentally estimated values of PPP as discussed above.

One can see that the VEH method with the original energy scale yields good agreement with "observed" values for both the bandwidth and the absolute energy of the π -band [18], although a contraction of the energy scale by a factor of 1.3 and a shift are required for a good overall fit of all valence states (see Fig. 1(d)). The CNDO/S3 method gives also a fairly good agreement once a 0.7 eV reduction of the calculated binding energies is applied. This shift is required for a good fit with the experimental results for benzene [6]. The ab-initio calculation produces a large π -bandwidth inconsistent with experiment. Upon contracting the energy scale by a factor of 1.34 and applying an appropriate shift a fairly good description of the shape of the DOVS over the whole valence region is obtained (Fig. 1(c)). The success of these calculations, although with some modifications, is encouraging for investigating the electronic structures of other polymers.

4. Concluding Remarks

In the present work UPS spectra of p-sexiphenyl and shorter oligomers have been presented. The good overall correspondence of the sexiphenyl spectrum with the reported XPS spectrum of PPP verifies that sexiphenyl is a good model compound for PPP. The observed fine structure caused by the levels derived from the benzene e_{1g} π -orbital have been successfully analyzed in a detailed way with the aid of theoretical band calculations by the VEH- and the CNDO/S3-method. In particular, the assignment of k-values to the observed energy levels by applying Eq. (3) allowed us to deduce experimental $E = E(k)$ dispersion relations for the uppermost π -bands of a PPP chain. The bandwidth of these bands and the ionization threshold energy for solid PPP were estimated to be 3.95 eV and 5.65 eV, respectively. The effect of nonplanarity in the molecular geometry on the electronic structure was elucidated by comparison to theoretical calculations.

We wish to emphasize that the technique of intramolecular band mapping described here which is based on the use of data from oligomers is almost unique to organic polymers. The molecules in the specimen need not to be oriented, but they should have the same number of units. Further, the inter-unit interaction should be one-dimensional and fairly well limited between the nearest neighbours. These conditions are often met in organic systems.

For inorganic compounds such as metals or semiconductors, it is difficult to prepare and characterize an aggregation of clusters with the same number of units. Furthermore, the interatomic interaction in inorganic systems is usually neither one-dimensional nor of short range. Consequently, for inorganic systems, band mapping usually requires single crystals and angle resolved photoemission [39].

Of course, angle resolved photoemission from oriented samples can also be applied successfully to investigate the intramolecular band dispersion of a polymer, as we have recently shown for $n\text{-CH}_3(\text{CH}_2)_{34}\text{CH}_3$ which is a good model compound of polyethylene [18]. The advantage of the present technique is that it does not require an oriented sample nor a sophisticated ARUPS instrument, provided that there is no overlap with other bands and that a fairly long oligomer is available. We anticipate that these techniques applied to other polymers, with proper choice of the method for each compound, will soon give us a detailed understanding of their intramolecular band dispersion and how the energy bands evolve from those of shorter compounds. Furthermore, the role of solid state polarization effects can be quantitatively assessed.

Acknowledgements

The authors are grateful to Dr. J.L. Brédas for detailed information on recent band calculations, and to Dr. J.P. Boutique for offering a preprint describing recent results. K.S. wishes to thank HASYLAB for a visitors fellowship, and U.K. thanks DAAD for financial support.

References

- 1 D.M. Ivory, G.G. Miller, J.M. Sowa, L.W. Shacklette, R.R. Chance, and R.H. Baughman, *J. Chem. Phys.* 71 (1979) 1506; L.W. Shacklette, R.R. Chance, D.M. Ivory, G.G. Miller, and R.H. Baughman, *Syn. Metals* 1 (1979) 307
- 2 N.N. Tyutyulkov and O.E. Polansky, *Z. Naturforsch.* A32 (1977) 490
- 3 M.W. Whangbo, R. Hoffmann, and R.B. Woodward, *Proc. Roy. Soc. (London)* A366 (1979) 23
- 4 P.M. Grant and I.P. Batra, *Syn. Metals* 1 (1979/1980) 193
- 5 J.J. Brédas, R.R. Chance, R. Silbey, G. Nicolas, and Ph. Durand, *J. Chem. Phys.* 77 (1982) 371; J.L. Brédas, private communication
- 6 W.K. Ford, C.B. Duke, and A. Paton, *J. Chem. Phys.* 78 (1983) 4734
- 7 J.P. Boutique, J. Riga, J.J. Verbist, J. Delhalle and J.G. Fripiat, private communication
- 8 J.L. Brédas, R. Silbey, D.S. Boudreaux and R.R. Chance, *J. Am. Chem. Soc.* 105 (1983) 6555
- 9 J. Riga, J.J. Pireaux, J.P. Boutique, R. Caudano, J.J. Verbist and Y. Gobillon, *Syn. Metals* 4 (1981) 99
- 10 G. Crecelius, J. Fink, J.J. Ritsko, M. Stamm, H.-J. Freund, and H. Gonska, *Phys. Rev.* B28 (1983) 1802
- 11 For a review, see G. Wegner, *Angew. Chem.* 20 (1981) 361
- 12 For example, J.P. Maier and D.W. Turner, *Faraday Disc. Chem. Soc.* 54 (1972) 149
- 13 For example, S. Hino, K. Seki, and H. Inokuchi, *Chem. Phys. Letters* 36 (1975) 335
- 14 N. Sato, K. Seki, and H. Inokuchi, *J. Chem. Soc. Faraday Trans 2* 77 (1981) 1621, and references therein
- 15 C.A. Feldmann, R. Engelhardt, T. Permien, E.E. Koch, and V. Saile, *Nucl. Instrum. Methods Phys. Res.* 208 (1983) 785
- 16 T. Hirooka, K. Tanaka, K. Kuchitsu, M. Fujihira, H. Inokuchi, and Y. Harada, *Chem. Phys. Letters* 18 (1973) 390
- 17 K. Seki and H. Inokuchi, *Chem. Phys. Letters* 89 (1982) 268
- 18 K. Seki, U.O. Karlsson, R. Engelhard, and E.E. Koch, *Chem. Phys. Letters* 103 (1984) 343
- 19 P.J.L. Baudour, Y. Delugeard, and H. Cailleau, *Acta Cryst.* B32 (1976) 150
- 20 K. Seki, H. Inokuchi, and Y. Harada, *Chem. Phys. Letters* 20 (1973) 197
- 21 W.D. Grobman and E.E. Koch, in *Photoemission in Solids*, ed. L. Ley and M. Cardona (Springer Verlag, Berlin, 1979) vol. 2, p. 261
- 22 For example, J.W. Rabalais, *Principles of Ultraviolet Photoelectron Spectroscopy* (Wiley, New York, 1979)
- 23 For example, E. Heilbronner and H. Bock, *Das HMO-Modell und seine Anwendung* (Verlag Chemie, Weinheim, 1970)
- 24 For example, C. Kittel, *Introduction to Solid State Physics*, 5th ed. (Wiley, New York, 1976)
- 25 J.J. Pireaux, S. Svensson, E. Basilier, P.-A. Marmqvist, U. Gelius, R. Caudano, and K. Siegbahn, *Phys. Rev.* A14 (1976) 2133
- 26 A. Alménningen, O. Bastiansen, and M. Traettberg, *Acta Chem. Scand* 12 (1958); *Tables of Interatomic Distances*, ed. L.E. Sutton (The Chemical Society, London, 1958)
- 27 A. Hargreaves and S.H. Rizui, *Acta Cryst.* 15 (1962) 365; J. Trotter, *Acta Cryst.* 14 (1961) 1135
- 28 H.M. Rietveld, E.N. Maslen, and C.J.B. Clews, *Acta Cryst.* B26 (1970) 693
- 29 Y. Delugeard, J. Desuche, and J.L. Baudour, *Acta Cryst.* B32 (1976) 702
- 30 S. Ramadas and J.M. Thomas, *J. Chem. Soc. Faraday Trans 2* 72 (1976) 1251
- 31 P.J.L. Baudour, Y. Delugeard, and H. Cailleau, *Acta Cryst.* B32 (1976)
- 32 C.B. Duke, A. Paton, W.R. Salaneck, H.R. Thomas, E.W. Plummer, A.J. Heeger, and A.C. McDiarmid, *Chem. Phys. Letters* 59 (1978) 146. We note that there is an error in their diagram both concerning the number of levels and the assignment of phases to the levels.
- 33 R. Boschi, E. Clar, and W. Schmidt, *J. Chem. Phys.* 60 (1974) 4406
- 34 S. Pignataro, V. Mancini, J.N. Ridyard, and H.J. Lempka, *J.C.S. Chem. Commun.* (1971) 142
- 35 S.X. Chen, K. Seki, N. Ueno, K. Sugita, S. Hashimoto, and H. Inokuchi, unpublished
- 36 K. Seki, unpublished
- 37 J. Tanaka, M. Tanaka, H. Fujimoto, M. Shimizu, N. Sato, and H. Inokuchi, *J. de Phys.* C3 (1983) 279
- 38 H. Shirakawa, F.J. Louis, A.G. McDiarmid, C.K. Chiang, and A.J. Heeger, *J.C.S. Chem. Commun.* (1977) 578
- 39 For example, E.W. Plummer and W. Eberhardt, *Adv. Chem. Phys.* 49 (1982) 533; F.J. Himpsel, *Advances in Physics* 32 (1983) 1
- 40 W. Schmidt, *J. Chem. Phys.* 66 (1977) 828

Table 1

Experimental binding energies for sexiphenyl and PPP relative to the vacuum level (in eV).

Feature in the UPS spectrum	Sexi-phenyl Solid (UPS)	Sexi-phenyl Gas (UPS)	Feature ^{a)} in the XPS spectrum	PPP ^{a)} Solid (XPS)	Assignment by VEH calculation ^{b)}
Threshold	5.9 ₀	7.2			
A	6.3 ₅	7.62	G'	6.5	$\pi(2b_1)^{c)}$
B	6.9 ₀	8.11			
C	7.6 ₀ ^{d)}	8.6			
D	8.1 ₃ ^{d)}	9.09	F'	8.1	$\pi(1a_2)^{c)}$
E	--- ₂ ^{e)}	9.4			
F	8.9 ₀ ^{e)}	9.9			
G	--- _{e)}	10.1			
H	--- _{e)}	10.9			
I	10.3	11.7	E'	10.3	$\sigma+\pi(1b_1)^{c)}$
J	11.0	12.1	D'	13.4	σ
K	13.0	14.0			
L	14.4	15.4	C'	17.5	σ
M	16.0				
N	17.6				
O	18.9		B'	21.9	2s σ
P	21.4		A'	25.0	2s σ

a) Ref. [9]. A work function of 4.5 eV is assumed for the conversion of the energy scale (see text)

b) Ref. [5].

c) Original benzene orbitals labelled in C_{2v} group symmetry. The long axis and short axis are z and y respectively.

d) Contains some contribution from E.

e) Observed only in the gas phase.

Table 2

Binding energies of the highest occupied orbital and the dominating main peak in the UPS spectra of p-polyphenylenes. P_+ and R_+ denote the gas to solid shifts of the threshold- and peak-energies, respectively.

Compound	highest occupied state				P_+	R_+	main peak		
	threshold		peak				solid	gas	R_+
	solid	gas	solid	gas					
Benzene	7.1 ^{a)}	9.25	8.1 ^{a)}	9.25	2.1	1.1	8.1 ^{a)}	9.25	1.1
p-Terphenyl	6.1 ^{b)}	7.8	6.6 ^{b)}	8.04	1.7	1.4	7.85 ^{b)}	9.03	1.2
p-Sexiphenyl	5.9	7.2	6.35	7.62	1.3	1.3	8.13	9.09	1.0
PPP ^{c)} (coplanar)	(5.65)	(6.75)	(6.10)	(7.2)	(1.1)	(1.1)	---	---	---
PPP ^{c)} (twisted)	(5.85)	(6.95)	(6.30)	(7.4)	(1.1)	(1.1)	---	---	---

a) Ref. [21] and [36].

b) Ref. [13].

c) Estimated from experimentally observed values. See text.

Table 3

Comparison of the calculated and observed bandwidth of the uppermost π -band and the energy of the highest occupied orbital in eV for PPP.

Method	width of the π -band (13+13')	HOMO energy
VEH ^{a)}	3.9	7.45
CNDO/S3 ^{b)}	3.3	8.5
ab initio ^{c)}	4.80	5.62
observed ^{d)}	3.9	7.2

a) Ref. [5].

b) Ref. [6].

c) Ref. [7].

d) Estimated from experimental values. See text.

Figure Captions

- Figure 1 Photoelectron spectra of sexiphenyl and PPP compared with theoretical density of the valence states (DOVS). (a) spectrum of solid sexiphenyl taken with a photon energy of 33 eV. (b) XPS spectrum of solid PPP by Riga et al. [9]. The energy axis is adjusted to fit the spectrum in (a). (c) DOVS of planar p-quarterphenyl (broken line) and PPP (solid line) by the CNDO/S3 method [6]. (d) DOVS of twisted ($\phi = 22.7^\circ$) PPP by the VEH method [5]. The intensity is corrected for the atomic photoionization cross-section at the $Al-K_{\alpha}$ XPS excitation energy. The energy axis is 1.3 times contracted and shifted in order to obtain an optimal fit with (a). (e) DOVS of planar p-quarterphenyl by ab-initio calculation [7]. The intensity is corrected for the XPS cross-section effects. The energy axis is 1.34 times contracted and shifted in order to obtain an optimal fit with (a).
- Figure 2 Gas phase HeI photoelectron spectra of p-sexiphenyl (a), p-quinquephenyl (b), p-quarterphenyl (c), p-terphenyl (d), biphenyl (e), and benzene (f).
- Figure 3 Low-binding-energy region of the photoelectron spectrum for gas phase and solid sexiphenyl.
- Figure 4 Evolution of the π -bands of p-phenylenes from the e_{1g} orbitals of benzene in the simple model. —: one of the degenerate e_{1g} orbitals (energy α) splits by the inter-ring interaction β . The origin of the energy scale is set at α . ---: The other orbital does not interact, resulting in a large density of valence states at α . At the right hand, the $E = E(k)$ dispersion relation of an infinite PPP chain is shown.
- Figure 5 Energy levels of benzene and p-phenylene oligomers observed by gas phase HeI photoelectron spectroscopy. - ' - : intense nonbonding π -electron peak ($1a_2$), —: split π -electron peak ($2b_1$) and ---: σ level.
- Figure 6 Experimental and theoretical $E = E(k)$ energy band dispersion relation for polyphenylenes. (a) Comparison of the experimental data with the simple model (Eq. (2)). Parameters $\alpha = 9.1$ eV

and $\beta = 1.0$ eV (solid) or $\beta = 0.8$ eV (gas) are used. (b) CNDO/S3 calculation for a PPP polymer ($\phi = 0^\circ$ and 23°) and a biphenyl molecule ($\phi = 0^\circ, 20^\circ,$ and 42°) [6]. (c) Comparison of the experimental data with the VEH calculation for a PPP chain ($\phi = 0^\circ, 22.7^\circ,$ and 42°) [5].

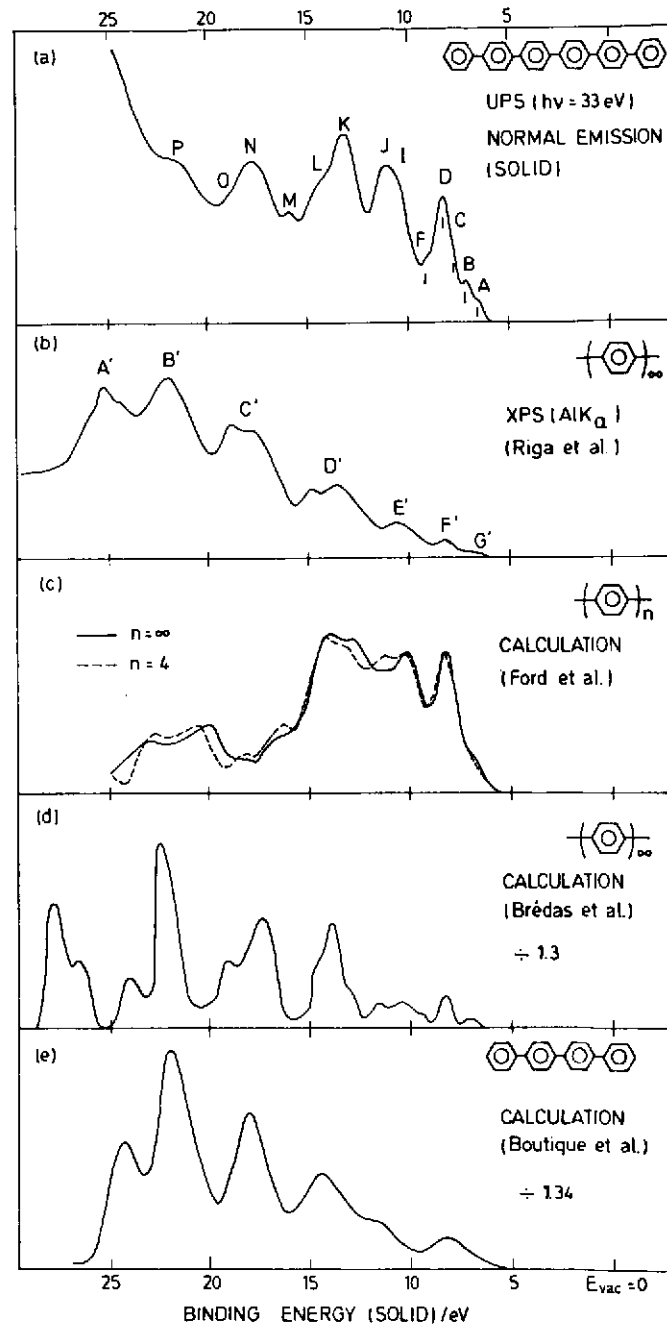
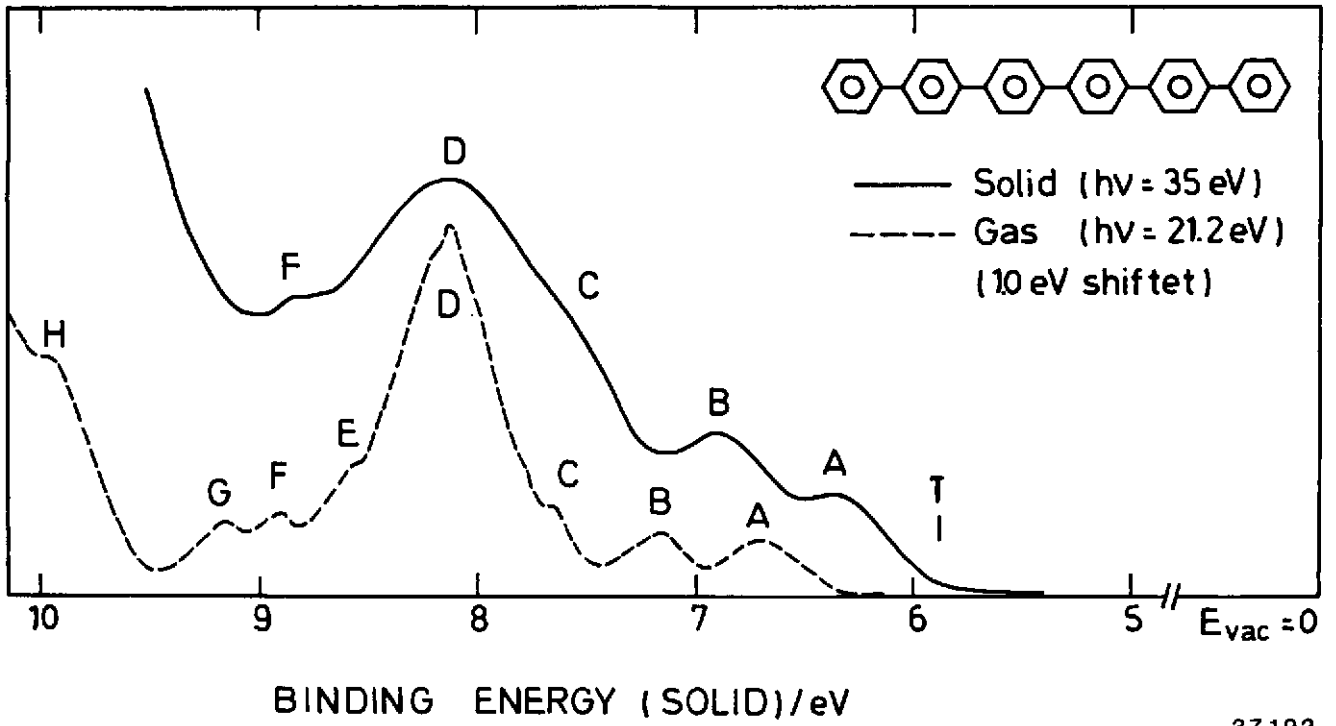


Fig. 1



37192

Fig. 3

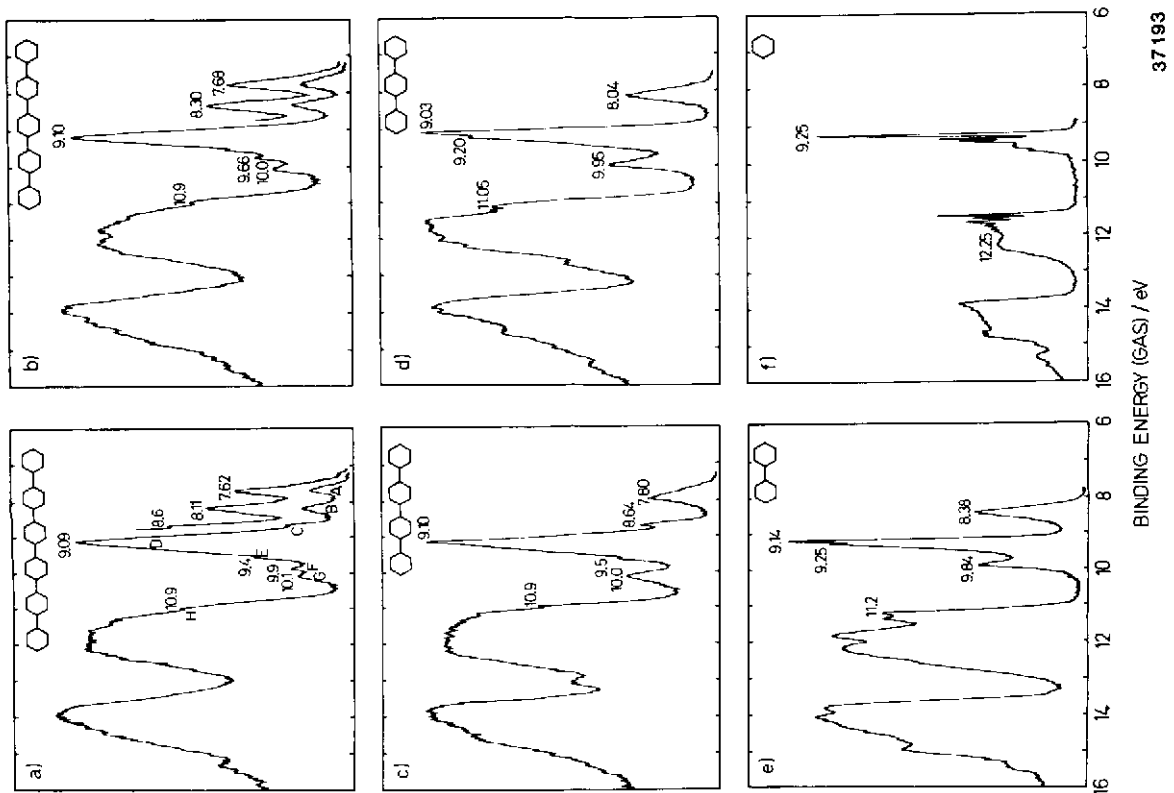


Fig. 2

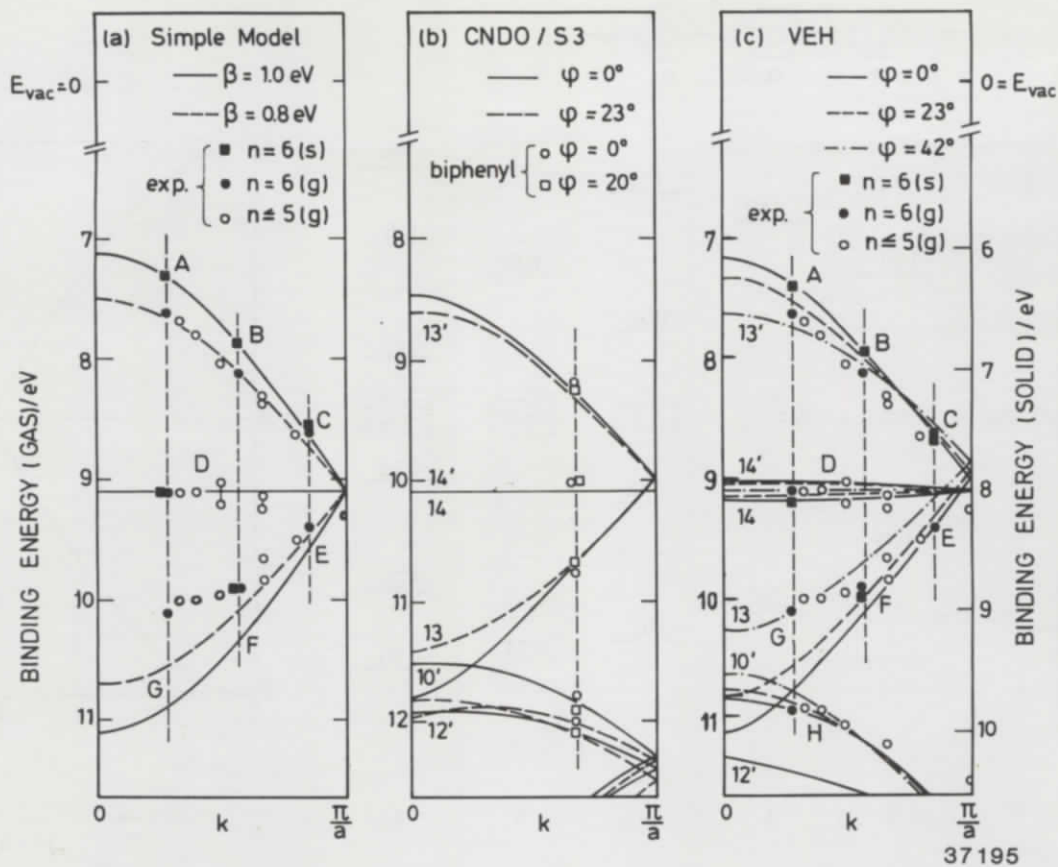


Fig. 6